2022

Development Of Novel Hybrid Battery Thermal Management System Coupling With Phase Change Material Under Fast Charging Conditions

Seunghoon Lee

Hoseong Lee

Development of Novel Hybrid Battery Thermal Management System coupling with Phase Change Material under Fast Charging Conditions

Seunghoon Lee[1], Hoseong Lee[2]*

[1]Department of Automotive Convergence, Korea University,
409 Innovation Hall Bldg., Anam-Dong, Sungbuk-Gu, Seoul, Republic of Korea
Tel: (02) 3290-3891, E-mail: aoliolas@korea.ac.kr

[2]Department of Mechanical Engineering, Korea University,
409 Innovation Hall Bldg., Anam-Dong, Sungbuk-Gu, Seoul, Republic of Korea
Tel: (02) 3290-3355, E-mail: hslee1@korea.ac.kr

ABSTRACT

In this study, a novel battery thermal management system (BTMS) coupled with phase change material (PCM) is proposed to improve its performance under fast charging conditions. A battery thermal model and two-phase PCM simulation model were developed and coupled with a liquid-cooling system. The developed model was validated using experimental data, and a parametric study was conducted by changing the parameters of the PCM and the operating conditions of the liquid-cooling system. The simulation results revealed that in the proposed system, the highest maximum temperature of the battery module was 38.4°C and the maximum temperature difference was 3.9°C during the charge–discharge cycle, and both these values were simultaneously maintained within the proper range of the battery cell. The aforementioned values were 13.2°C and 10.8°C lower compared with the corresponding values for the conventional liquid-cooling method. In addition, through the optimal operating conditions, sufficient heat dissipation was achieved while shortening the operating time of the liquid-cooling system by 12.4% of the total time. Finally, the latent heat of the PCM was recovered sufficiently during the cycle. Therefore, we claim that the proposed BTMS is not only effective in terms of its cooling performance but also sufficiently usable in the continuous cycle.

1. INTRODUCTION

Lithium-ion batteries are widely used because of advantages such as high specific energy, high working voltage, non-memory effect, and long endurance. As the energy density of the battery cell increases and more battery cells are concentrated in a limited space, the heat generation of the cells increases and the temperature difference between the cells also increases. But the performance of lithium-ion batteries is greatly affected by operating temperature and temperature uniformity. The proper operating temperature should be maintained between 15°C and 45°C, and the temperature difference between cells should be maintained within 5°C (Pesaran et al., 2002). In a high temperature environment, the problem as accelerated battery performance degradation, thermal runaway, abnormal temperature distribution within battery cells occurs, and in a low-temperature environment, the problem as reduced battery power and capacity fade due to lithium plating during charging and discharging occurs (zhang et al., 2020). Therefore, an efficient battery thermal management system is needed. Among the various battery thermal management system, in such a situation, in case of the air cooling method, the thermal conductivity and heat capacity of air are too low. In case of the liquid cooling system, the difference between the inlet and outlet temperature of the coolant occurs first. Also, the bottom cooling method applied to electric vehicles recently causes the temperature difference between the upper and lower parts of the battery module because the cooling plate is located at the bottom of the battery pack to prevent contact with the battery cell. Such temperature difference causes problems such as thermal stress, capacity loss, increase in impedance, and deformation of the battery cell. To solve the problem of temperature difference between cells, the PCM cooling method is considered. The PCM cooling method can reduce the temperature difference through a phase change process that occurs under a constant temperature. and since it is a passive cooling method that does not require additional energy consumption such as a heater or a chiller, it can reduce power consumption when applied to the conventional system. Because of these advantages, recent studies on PCM cooling method have been conducted. In the PCM cooling method, the heat absorbed by the PCM must eventually be dissipated, so an air cooling

method or a liquid cooling method must be combined with the PCM. So, research on the PCM cooling method combined with the secondary cooling method which serves to re-solidify the melted PCM has been activated recently. Kong et al. (2020) proposed a system wherein five S-shaped aluminum tubes were installed in a PCM, which was placed between cylindrical battery cells from top to bottom and a liquid cooling strategy for controlling the velocity and inlet temperature of the coolant during continuous cycle for different ambient temperatures. Liu et al. (2021) and Hekmat et al. (2020) experimentally investigated a thermal management system comprising a PCM and liquid-cooling pipes between battery cells. To solve the problem of low thermal conductivity of a PCM and enhance the heat transfer efficiency, Liu et al. (2021) conducted a parametric study for a system using helical liquid channels, instead of conventional straight channels, among battery cells, and Gao et al. (2022) proposed a system with double-s-shaped micro-channels between prismatic lithium-ion batteries. A literature review conducted as part of this study revealed that studies on BTMSs with PCMs are not numerous. Moreover, it is difficult to find relevant studies on the practical application of PCMs to battery modules under fast charging conditions while considering both the maximum temperature and maximum temperature difference. In addition, when a PCM is applied to the battery thermal management module, the system becomes oversized. This is primarily owing to the low thermal conductivity of the PCM and the complicated heat sink device structure. Therefore, the current study focuses on proposing a novel battery thermal management module with a PCM under fast charging conditions. Sufficient heat dissipation performance improvement can be achieved via a compact design of the battery thermal management module. A battery thermal model and PCM model were first developed, and based on the models validated through experiments, a parametric study was conducted by changing the parameters of the PCM and operating conditions to realize the sensitivity of the selected parameters and determine the optimal conditions.

2. DESIGN DESCRIPTION

A battery thermal management system (BTMS) is newly proposed with a liquid bottom cooling plate, aluminum fins and pouches containing PCM as shown in Fig. 1. The PCM pouch is in contact with one side of the battery cell, and the aluminum fin is in contact with the other side. The battery cell considered in this study is the high-energy-density of lithium nickel manganese cobalt (LiNiMnCo) pouch-type Li-ion polymer battery (Kokam, SLPB75106205) with the size of 188 mm(length) X 100 mm(width) X 8 mm(thickness). The nominal capacity of the battery is 16 Ah, and the nominal voltage of the battery is 3.7 V. For the PCM, n-octadecane is used. After putting the PCM in a pouch made of polyethylene, it is sealed to make a PCM pouch. Fig. 1 (b) shows a battery module in which 8 sets of the battery cell, PCM pouch, and aluminum fin are included with the cooling plate. The aluminum fins and the cooling plate located below are connected through a thermal pad, which can reduce the thermal resistance of air. The size of cooling plate located below is 8 mm(length) X 100 mm(width) X 188 mm(thickness), and there are 3 straight flow channels with both inlet size and outlet size of 4 mm(length) X 4 mm(width). The cooling plate is made of aluminum, and water is used as the coolant. All three flow inlets and flow outlets are on the same direction, respectively.

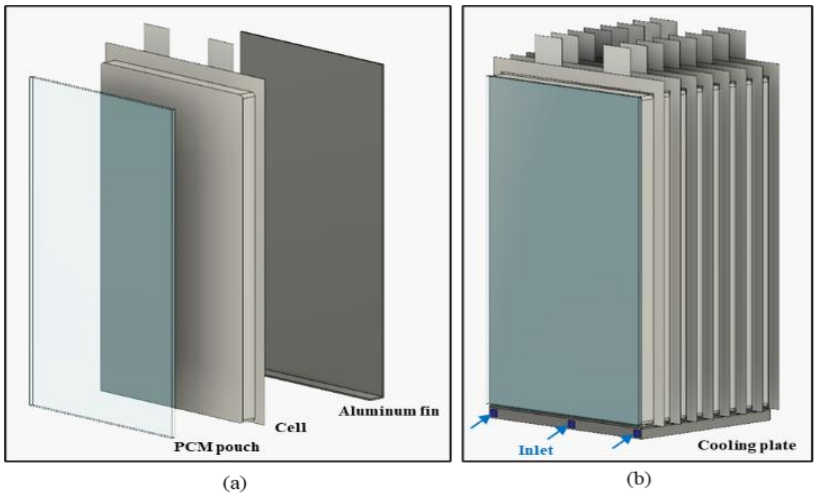

Figure 1: Schematic diagram of the battery module integrated with aluminum fins, PCM pouches, and cooling plate

3. MODEL DEVELOPMENT

3.1 Battery thermal model

The energy conservation equation of the battery cell can be written as Eq. (1).

$$\rho_b C_{p,b} V \frac{\partial T}{\partial t} = \frac{\partial}{\partial x}\left(k_{x,b}\frac{\partial T}{\partial x}\right) + \frac{\partial}{\partial y}\left(k_{y,b}\frac{\partial T}{\partial y}\right) + \frac{\partial}{\partial z}\left(k_{z,b}\frac{\partial T}{\partial z}\right) + \dot{Q}_{gen} - \dot{Q}_{dis} \quad (1)$$

Where x, y, z are the coordinates used in the system. ρ_b, $C_{p,b}$, V are density, specific heat, and volume of the battery cell, respectively. T is the temperature of the battery cell, $k_{x,b}$ and $k_{y,b}$ are the in-plane thermal conductivities and $k_{z,b}$ is the through-plane thermal conductivity of the battery cell. The right-hand side of Eq. (1) is consisted of the heat generation ($\dot{Q}_{gen}$) and heat dissipation ($\dot{Q}_{dis}$). First, heat generation ($\dot{Q}_{gen}$) is expressed as follows.

$$\dot{Q}_{gen} = \dot{Q}_{irr} + \dot{Q}_{rev} = I(V_{OC} - V) - IT\frac{dV_{OC}}{dT} = I(V_{OC} - V) - T\Delta S\frac{I}{nF} \quad (2)$$

Where I, V_{OC}, V are current, open circuit voltage, and cell voltage, respectively. And T, n, F each represent battery temperature in Kelvin, number of electrons, and Faraday constant. ΔS is the entropy change and the value of the entropy change for NMC type battery cell is presented by Wei et al. (2016). The heat generation ($\dot{Q}_{gen}$) can be derived adding the irreversible joule heat due to overpotential which is the difference between the operating battery voltage (V) and open-circuit voltage (V_{OC}) and the reversible entropic heat due to entropy change(ΔS) between cathode and anode of the battery cell during operation. The current (I) and the operating cell voltage (V) is measured from the experiment while charging and discharging. The open-circuit voltage (V_{OC}) is the electrical potential difference when an external load is not connected, which varies according to the state of charge (SOC) of the battery. Therefore, a separate experiment should be conducted to derive V_{OC} for SOC. Experiments to measure V_{OC} will be introduced later in section 4. And the values of entropy change (ΔS) also vary depending on the state of charge (SOC) like V_{OC}. The state of charge (SOC) is calculated as follows.

$$SOC(t) = SOC(t-1) - \int \frac{I}{3600 \cdot Ca_b} dt \quad (3)$$

Where the I and Ca_b is the current and the capacity of the battery cell which is 16 Ah. And the heat dissipation ($\dot{Q}_{dis}$) is expressed as follows.

$$\dot{Q}_{dis} = A_{tot} \cdot h_{total} \cdot (T_{cell} - T_{amb}) \quad (4)$$

Where A_{tot}, h_{total} indicate the total heat transfer area in contact with the ambient air and overall heat transfer coefficient. T_{cell}, T_{amb} is the temperature of battery cell and ambient air, respectively. $\dot{Q}_{dis}$ is the heat loss that dissipates to the surrounding environment and the overall heat transfer coefficient is determined from the experiment. The heat transfer coefficients for experimental cases are computed as 2.3 $W \cdot m^{-2} \cdot K^{-1}$ and then used for the validation in section 4.

3.2 PCM model

In the numerical simulation for PCM, enthalpy-porosity technique is used to simulate the solid-liquid phase change modeling. In this technique, the melting interface is not tracked explicitly. Instead, the PCM domain is modeled as a mushy region in which the liquid fraction is from 0 to 1. The liquid fraction indicates the fraction of the cell volume which is in liquid state. The mushy zone is a "pseudo" porous medium in which the porosity increases from 0 to 1 as the material melts. So, the porosity in each cell is set equal to the liquid fraction in that cell. The heat transfer inside the PCM is divided into sensible heat and latent heat. The governing equations that are solved in the PCM domain are as follows.

Continuity equation

$$\frac{\partial \rho_{PCM}}{\partial t} + \nabla \cdot (\rho_{PCM}\overrightarrow{v_{PCM}}) = 0 \quad (5)$$

Momentum balance equation

$$\rho_{PCM}\frac{\partial\overrightarrow{v_{PCM}}}{\partial t}+\rho_{PCM}(\overrightarrow{v_{PCM}}\cdot\nabla)\overrightarrow{v_{PCM}}=-\nabla\mathrm{P}+\nabla\cdot(\mu_{PCM}\nabla\overrightarrow{v_{PCM}})+\rho_{PCM}\vec{g}\ +S \tag{6}$$

Energy equation

$$\rho_{PCM}\frac{\partial H}{\partial t}+\nabla(\rho_{PCM}\overrightarrow{v_{PCM}}H)=\nabla\cdot(k_{PCM}\nabla T_{PCM}) \tag{7}$$

where ρ_{PCM}, k_{PCM}, k_{PCM}, S, $\overrightarrow{v_{PCM}}$, T, $\nabla\mathrm{P}$, $\vec{g}$, H is the density, thermal conductivity, dynamic viscosity, momentum source term, fluid velocity, temperature, pressure, gravitational acceleration, and the specific enthalpy, respectively. The momentum source term is expressed as follows.

$$S=\frac{(1-\beta)^2}{(\beta^3+\varepsilon)}A_{mush}(\overrightarrow{v_{PCM}}-\overrightarrow{v_{PCM,p}}) \tag{8}$$

Where $\overrightarrow{v_{PCM,p}}$ is the pull velocity of PCM. A_{mush} is 10^5 of the consecutive number in the mushy region which determines the damping of the velocity during melting. ε is a small constant number to avoid division by zero, 0.001. The momentum source term shows a velocity damping in the transition region between solid and liquid regions. It makes the velocity to be equal to zero at the solid region and maximum at the liquid region. The A_{mush} constant indicates the magnitude of damping. And the pull velocity is the velocity at which the solid is pulled out of the domain. The enthalpy of the PCM is expressed as follows.

$$H=h_s+\Delta H \tag{9}$$

$$h_s=\int_{T_0}^{T}C_{p,PCM}\,dT \tag{10}$$

$$\Delta H=\beta L \tag{11}$$

$$\beta=\begin{cases}0\ (T<\ T_s)\\ \dfrac{T-T_s}{T_l-T_s}(T_s<T<T_l)\\ 1\ (T>T_l)\end{cases} \tag{12}$$

Where $C_{p,PCM}$ is the specific heat of PCM. β is liquid fraction of PCM. L is the latent heat of phase change. T_s is the solid melting temperature of the PCM, and T_l is the liquid melting temperature of PCM.

4. EXPERIMENT FOR VALIDATION

All experiments are carried out while maintaining the ambient temperature constant at 20°C in the environmental test chamber. Then the single cell is carried out in two situations, 3C charging and 0.5C discharging, in order to obtain temperature data, five thermocouples are attached to the cell and the temperature is measured. One thermocouple is attached to the center of the battery cell and the other four are attached near each vertex. The temperature obtained through thermocouples is collected with the data acquisition system. Next, in order to validate the PCM model, a PCM pouch is manufactured. n-octadecane is used for the PCM. In order to fabricate the PCM pouch, the PCM is first melted in an ambient air at 30°C higher than melting temperature of 27.7°C in the environmental test chamber. And the required amount of PCM is calculated based on the amount of heat generation during 3C charging which has the highest amount of heat generation. After that, when the PCM melts by the ambient temperature and the PCM is in liquid state, the PCM is measured as much as the corresponding weight, and then it is put in a polyethylene pouch. After attaching the manufactured PCM pouch to one side of the battery cell, the test is conducted in a continuous cycle of 3C charging and 0.5C discharging. A rest time of 10 minutes is put between charging and discharging. Between the PCM pouch and the battery cell, five thermocouples are attached to

measure the temperature as in the previous single battery experiment. And the overall heat transfer coefficient in the simulation for validation is set through the method in the previous section 3.1. Fig. 2 and Fig. 3 compares the temperature data measured with a thermocouple and the result through simulation. It is confirmed that the numerical and the experimental results are consistent with each other within an average error of 1.5% and 2.1% in 3C charging and 0.5C discharging. and an average error of 1% in experiment with battery cell with attached PCM pouch. Therefore, small errors are shown, so the accuracy of the simulation model is confirmed.

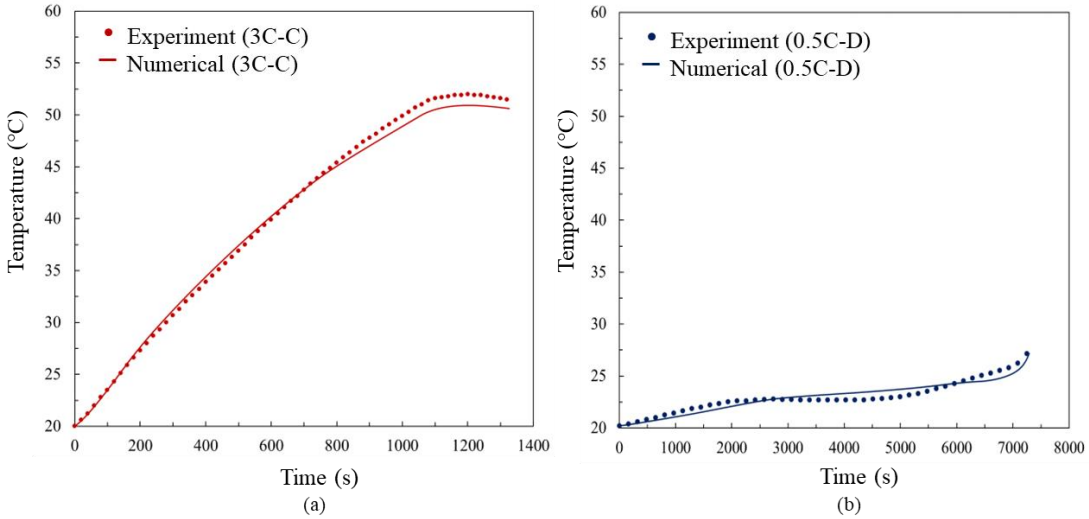

Figure 2: Comparison of experimental and numerical results during 3C charging and 0.5C discharging

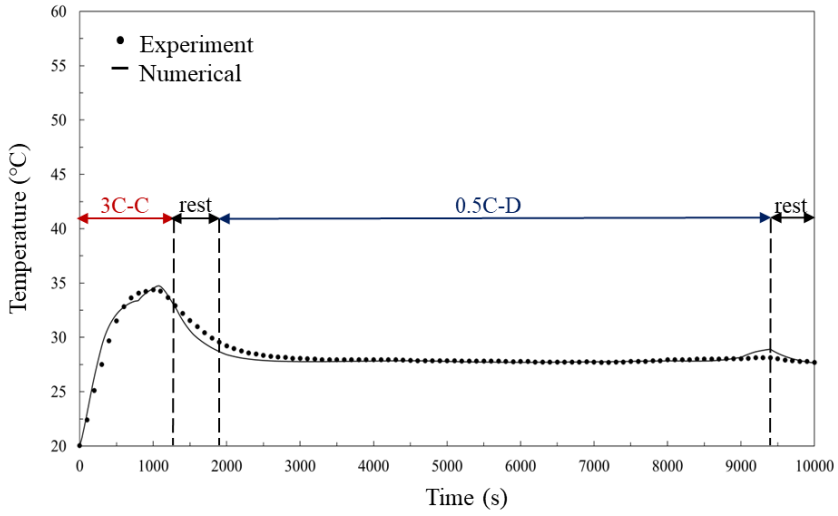

Figure 3: Comparison of experimental and numerical results during the charge-discharge cycle with PCM

5. RESULT AND DISCUSSION

5.1 Thermal performance of the proposed system

To analyze the thermal performance of the proposed system, simulations are conducted for three thermal management methods: air cooling method, liquid cooling method, and the proposed system. The simulation is conducted for the case of 3C charging, and both the temperature of ambient air and inlet are set to 25°C. The inlet velocity is set to 0.2 $m \cdot s^{-1}$ for liquid cooling method and 0 $m \cdot s^{-1}$ for the proposed system. In the case of the proposed system, n-eicosane having a melting temperature of 36.1°C is used as PCM between the battery cells, and a PCM pouch with a thickness of 2 mm is inserted. As shown in Fig. 4 and Fig. 5, in the proposed system, the maximum temperature and the maximum temperature difference become constant when the temperature of the battery cell approaches the melting

temperature of the PCM. And since the highest maximum temperature and the maximum temperature difference is 38.6°C and 1.7°C during 3C fast charging, it satisfies the target of the optimal operating temperature and the temperature difference between cells. However, in this simulation of the proposed system, the inlet velocity is 0 $m \cdot s^{-1}$. So, it only confirms that the temperature of the battery cell can be sufficiently controlled during 3C fast charging. It is still unknown whether the proposed system will be able to sufficiently recover the latent heat of the molten PCM, and thus successfully control the temperature of the battery module in a continuous cycle. Therefore, in the following sections, simulations including consideration of such continuous cycle are performed.

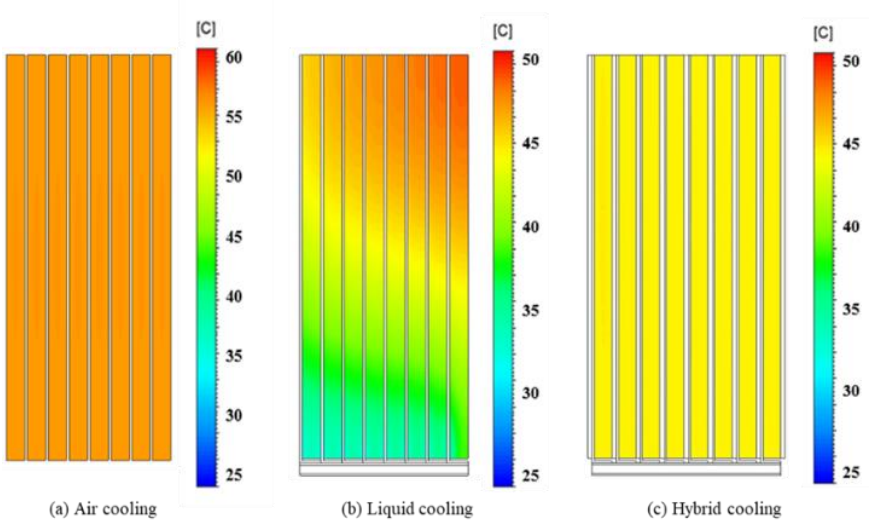

Figure 4: Temperature contours according to thermal management methods at the end of 3C charging

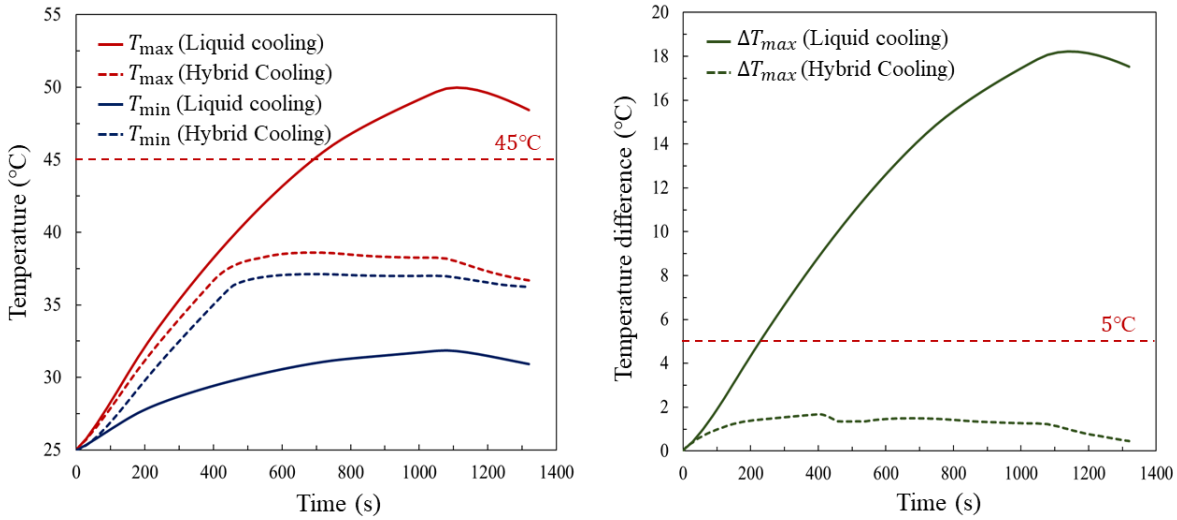

Figure 5: T_{max}, T_{min} and ΔT_{max} versus time under liquid cooling and hybrid cooling during 3C charging

5.2 Effect of PCM melting temperatures

It is important to select a PCM with an appropriate melting temperature for effective battery cooling. In this study, three types of PCM are selected: n-octadecane with a melting temperature of 27.7°C, n-eicosane with a melting temperature of 36.1°C, and n-docosane with a melting temperature of 44°C. The ambient temperature is set to 25°C, and the inlet velocity is set to 0.1 m·s-1. A simulation is performed for a 3C charge-0.5C discharge cycle, and 10 minutes rest time is put between charging and discharging. As shown in Fig. 6 (a), during 3C fast charging, the maximum temperature increased with a similar slope in all three cases of n-octadecane, n-eicosane, and n-docosane until the melting temperature of PCM. And then, when the PCM starts to melt, the temperature increase gradient begins to decrease significantly. In the case of the n-docosane, the highest maximum temperature of the battery module

during 3C charging is 45.7°C. Therefore, n-docosane is not suitable because the maximum temperature exceeds the proper operating temperature of 45°C. In addition, one of the important points in the PCM cooling method combined with liquid cooling method is that the latent heat of PCM must be recovered so that it can be used in the continuous cycle. As shown in Fig. 6 (b), in the case of n-eicosane and n-docosane, PCM completely recovers to a solid state as the liquid fraction of PCM reaches 0 in about 2900 s and 5590 s immediately after the end of fast charging. However, in the case of n-octadecane, which has a melting temperature of 27.7°C, the latent heat of PCM is not fully recovered with a liquid fraction of 0.88 until 10000 s. This is because there is not much difference between melting temperature of PCM and coolant temperature, so sufficient heat dissipation does not occur during the phase change section of n-octadecane. Therefore, n-eicosane with a melting temperature of 36.1°C is judged to be an appropriate PCM in the battery cooling module, and in the following simulations, it is used.

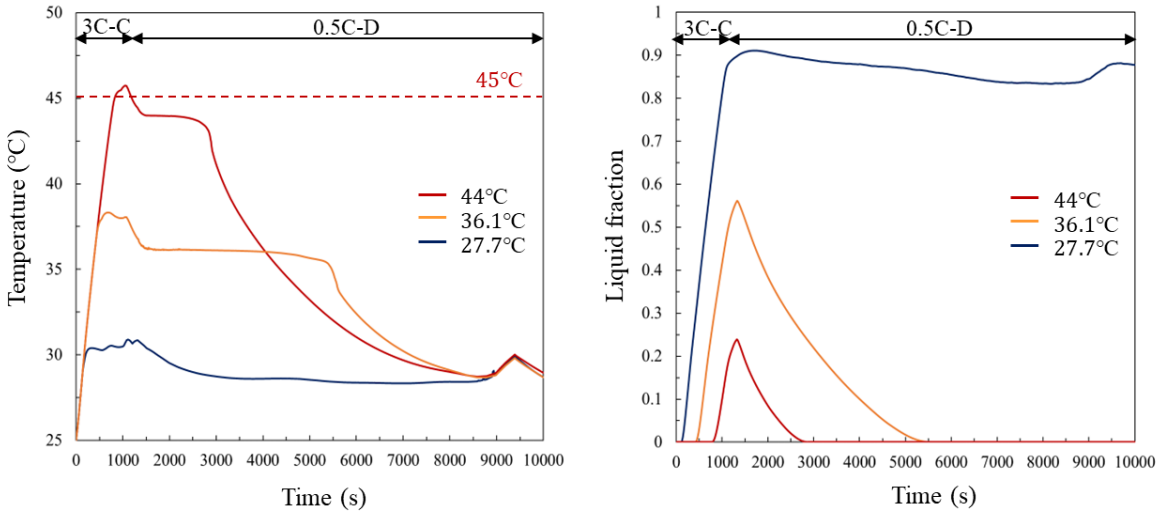

Figure 6: T_{max} and liquid fraction of the battery module versus time under different melting temperature

5.3 Effect of PCM thickness

An appropriate PCM thickness that can sufficiently control the battery cell temperature in the charge-discharge cycle is important because effective heat dissipation can be achieved without additional power consumption. The PCM thickness is simulated for a total of 4 cases: 0.5 mm, 1 mm, 2 mm, and 3 mm. At this time, the inlet temperature and the ambient temperature are set to 25°C as in the previous section, and the inlet velocity is set to 0.2 $m \cdot s^{-1}$ under 3C charging. As shown in Fig. 7 (a), when the thickness is between 0.5 mm and 2 mm, the maximum temperature and maximum temperature difference are greatly reduced as the thickness of the PCM increases. However, at the thickness of 2 mm or more, the decrease in the maximum temperature and the maximum temperature difference is lowered. In Fig. 7 (b), if the thickness of the PCM is not sufficient to absorb the heat generation of the battery cell, a section in which the maximum temperature difference is kept constant appears shortly, and then the maximum temperature difference begins to increase again. Therefore, 2 mm is selected as an appropriate PCM thickness. However, as shown in Fig. 7 (a), even when the thickness of 2mm is applied, the highest maximum temperature difference is 7.6°C, which is higher than the target of 5°C. Therefore, the optimal operating conditions such as the inlet velocity and inlet temperature of the liquid cooling system should be dealt with in the following sections.

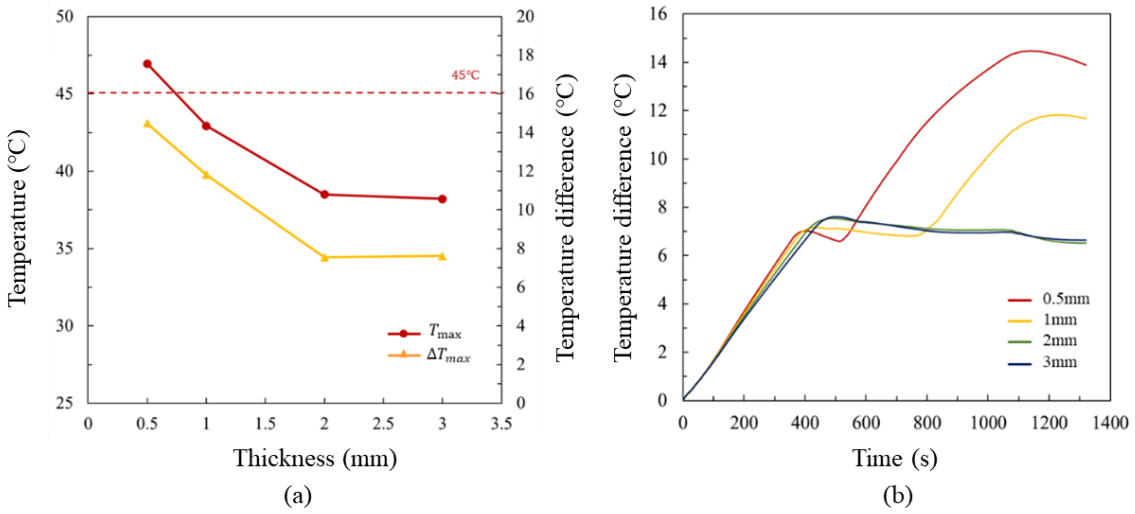

Figure 7: (a) T_{max} and ΔT_{max} under different PCM thickness, (b) ΔT_{max} versus time

5.4 Effect of operating conditions

In order to consider practical application, the charge-discharge cycle is divided into two sections, "During fast charging" and "After fast charging". In "During fast charging" section, 3C charging is considered, and in "After fast charging" section, 10 minutes rest-0.5C discharge-10 minutes rest is considered. Then the operating conditions such as the inlet velocity and inlet temperature are set differently for each section. Simulations are performed for inlet velocities of 0 m·s^{-1}, 0.1 m·s^{-1}, 0.2 m·s^{-1}, 0.3 m·s^{-1}, 0.4 m·s^{-1}, and 0.5 m·s^{-1}. As shown in Fig. 8, when the inlet velocity is 0 m·s^{-1}, the liquid fraction is 0.76, indicating that PCM is still in the phase change section. When the inlet velocity is 0.1 m·s^{-1}, 0.2 m·s^{-1}, 0.3 m·s^{-1}, 0.4 m·s^{-1}, and 0.5 m·s^{-1}, the latent heat of PCM is sufficiently recovered well before the end of the charge-discharge cycle. But, when the inlet velocity exceeds 0.2 m·s^{-1}, the improvement of the battery module cooling performance decreases as the inlet velocity increases. Therefore, the inlet velocity in the "After fast charging" section is selected as 0.2 m·s^{-1}.

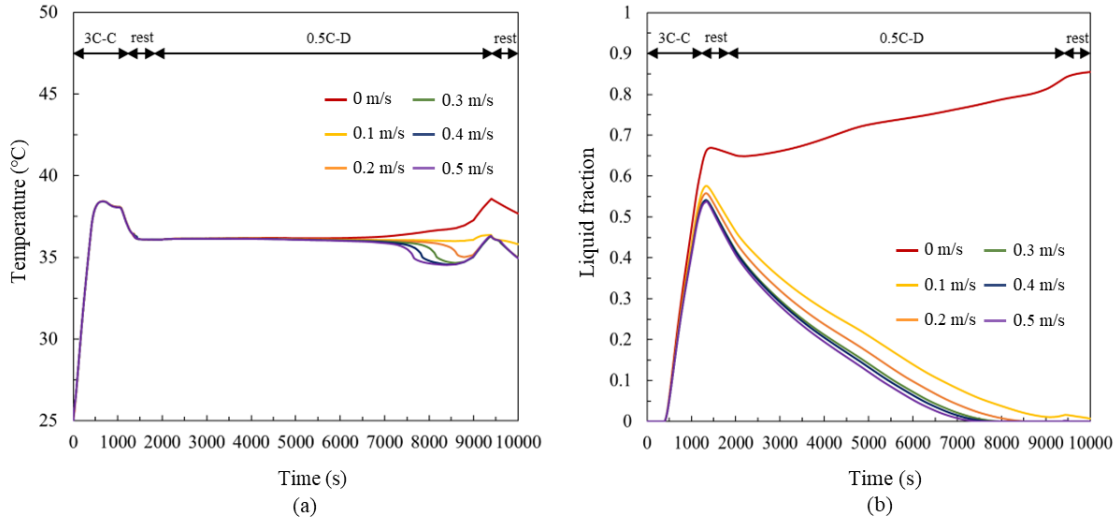

Figure 8: T_{max} and liquid fraction versus time under different inlet velocity during charge-discharge cycle

Lastly, the inlet temperature is important in recovering the latent heat of PCM. In the bottom liquid cooling method, the temperature of the lower part of the battery module is inevitably affected greatly by inlet temperature than the upper part. Therefore, the temperature of the cooling water is set at 31°C to be as low as about 5°C from the melting temperature of PCM. In addition, to reduce power consumption, on-off control is conducted to prevent the liquid cooling system from operating when PCM is completely in solid state. As result, as shown in Fig. 9, the maximum

temperature of the battery cell is continuously maintained below the target of 45°C during the charge-discharge cycle, and the maximum temperature difference is also maintained below 5°C. The liquid fraction of PCM is also about 0.006 right after the end of the cycle, confirming that the proposed system can be used for continuous cycles.

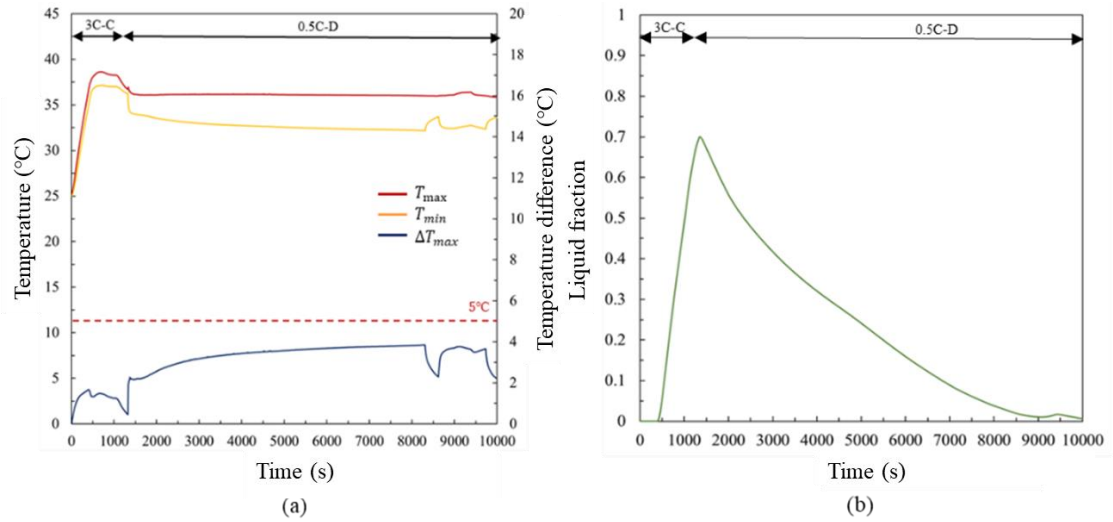

Figure 9: T_{max}, T_{min}, ΔT_{max}, and liquid fraction when applied optimal design parameters

6. CONCLUSIONS

A novel BTMS that combines a PCM pouch and bottom liquid cooling method through aluminum fin has been proposed to solve the problems of the convectional liquid cooling. The battery thermal model and the two-phase CFD simulation model to predict the phase change material are developed, and the developed model is validated through comparison of experimental values and numerical results. The parametric study by changing the parameters of PCM such as the thickness and melting temperature and optimum operating conditions of the liquid cooling system such as inlet velocity and its temperature is conducted. As a result, in terms of the melting temperature of PCM, n-eicosane with melting temperature of 36.1°C is selected. In terms of thickness, the thickness of 2 mm is selected as an appropriate value because PCM in the upper part did not become completely liquid state immediately after 3C fast charging. Afterwards, in terms of operating conditions, the entire charge-discharge cycle is largely divided into two sections, “During fast charging” and “After fast charging”, and simulations are conducted separately. An inlet velocity of 0.2 m·s-1 is selected in consideration of the degree of improvement in cooling performance according to the inlet velocity and the power consumption. In addition, to keep the maximum temperature difference below the target of 5°C, the inlet temperature is selected as 31°C, which is about 5°C lower than the melting temperature of n-eicosane. As a result, in the charge-discharge cycle of 3C charge-10 minutes rest-0.5C discharge-10minutes rest, the maximum temperature is less than the target point of 45°C, the maximum temperature difference is less than the target point of 5°C, and the liquid fraction of PCM is also 0.006 after the end of the cycle so that it is confirmed that it is sufficiently usable even in the subsequent cycle.

NOMENCLATURE

Al	aluminum	(-)
c-rate	current-rate	(C)
c_p	specific heat	(kJ·kg^{-1}·K^{-1})
h	cooling coefficient	(W·m^{-2}·K^{-1})
I	current	(A)
K	thermal conductivity	(W·m^{-2}·K^{-1})
m	mass	(kg)
NMC	nickel manganese cobalt	(-)
OCV	open-circuit voltage	(-)
$\dot{Q}$	heat generated or transferred	(W)

Re	Reynolds number	(-)
SOC	state of charge	(-)
t	time	(s)
T	Temperature	(℃)
Δt	timestep	(s)

Subscript

amb	ambient
cell	battery cell
gen	generation
i	initial
dis	dissipation
surr	surface

REFERENCES

Pesaran, A. A. (2002). Battery thermal models for hybrid vehicle simulations. Journal of power sources, 110(2), 377-382.

Zhang, L., Zhao, P., Xu, M., & Wang, X. (2020). Computational identification of the safety regime of Li-ion battery thermal runaway. Applied Energy, 261, 114440.

Shi, W., Zheng, J., Xiao, J., Chen, X., Polzin, B. J., & Zhang, J. G. (2016). The effect of entropy and enthalpy changes on the thermal behavior of Li-Mn-rich layered composite cathode materials. Journal of The Electrochemical Society, 163(3), A571.

Kong D, Peng R, Ping P, Du J, Chen G, Wen J. (2020). A novel battery thermal management system coupling with PCM and optimized controllable liquid cooling for different ambient temperatures. Energy Conversion and Management, 204.

Liu Z, Huang J, Cao M, Jiang G, Yan Q, Hu J. (2021). Experimental study on the thermal management of batteries based on the coupling of composite phase change materials and liquid cooling. Applied Thermal Engineering, 185.

Hekmat S, Molaeimanesh GR. (2020). Hybrid thermal management of a Li-ion battery module with phase change material and cooling water pipes: An experimental investigation. Applied Thermal Engineering, 166.

Liu H, Ahmad S, Shi Y, Zhao J. (2021). A parametric study of a hybrid battery thermal management system that couples PCM/copper foam composite with helical liquid channel cooling. Energy, 231.

Gao Z, Deng F, Yan D, Zhu H, An Z, Sun P. (2022). Thermal performance of thermal management system coupling composite phase change material to water cooling with double s-shaped micro-channels for prismatic lithium-ion battery. Journal of Energy Storage, 45.

ACKNOWLEDGEMENT

This research was supported by the program of the National Research Foundation of Korea (NRF-2019R1C1C1011195)